ACCOUNTS
of chemical research

Designed CVD Growth of Graphene via Process Engineering

KAI YAN,[†,‡] LEI FU,[†,§] HAILIN PENG,[†] AND ZHONGFAN LIU*[,†]

[†]*Center for Nanochemistry, Beijing National Laboratory for Molecular Sciences (BNLMS), State Key Laboratory for Structural Chemistry of Unstable and Stable Species, College of Chemistry and Molecular Engineering, Peking University, Beijing 100871, P.R. China,* [‡]*Department of Materials Science and Engineering, Stanford University, Stanford, California 94305, United States, and* [§]*College of Chemistry and Molecular Sciences, Wuhan University, Wuhan 430072, P.R. China*

RECEIVED ON FEBRUARY 27, 2013

CONSPECTUS

Graphene, the atomic thin carbon film with honeycomb lattice, holds great promise in a wide range of applications, due to its unique band structure and excellent electronic, optical, mechanical, and thermal properties. Scientists are researching this star material because of the development of various emerging preparation techniques, among which chemical vapor deposition (CVD) has received the fastest advances in the past few years. For the CVD growth of graphene, the ultimate goal is to achieve the highest quality in the largest scale and lowest cost with a precise control of layer thickness, stacking order, and crystallinity. To meet this goal, researchers need a comprehensive understanding and effective controlling of the growth process, especially to its elementary steps.

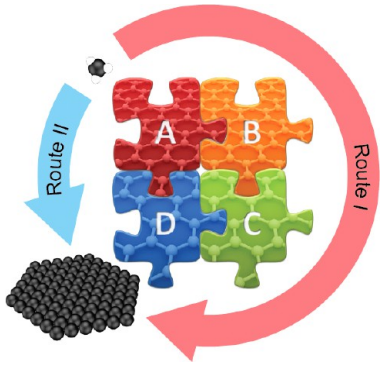

In this Account, we focus on our recent progresses toward the controlled surface growth of graphene and its two-dimensional (2D) hybrids via rational designs of CVD elementary processes, namely, process engineering. A typical CVD process consists of four main elementary steps: (A) adsorption and catalytic decomposition of precursor gas, (B) diffusion and dissolution of decomposed carbon species into bulk metal, (C) segregation of dissolved carbon atoms onto the metal surface, and finally, (D) surface nucleation and growth of graphene. Absence or enhancement of each elementary step would lead to significant changes in the whole growth process. Metals with certain carbon solubility, such as nickel and cobalt, involve all four elementary steps in a typical CVD process, thus providing us an ideal system for process engineering. The elementary segregation process can be completely blocked if molybdenum is introduced into the system as an alloy catalyst, yielding perfect monolayer graphene almost independent of growth parameters. On the other hand, the segregation-only process of predissolved solid carbons is also capable of high-quality graphene growth. By using a synergetic Cu−Ni alloy, we are able to further enhance the control to such a segregation technique, especially for the thickness of graphene. By designing a cosegregation process of carbon atoms with other elements, such as nitrogen, doped graphene could be synthesized directly with a tunable doping profile.

Copper with negligible carbon solubility provides another platform for process engineering, where both carbon dissolution and segregation steps are negligible in the CVD process. Carbon atoms decomposed from precursors diffuse on the surface and build up the thermodynamically stable honeycomb lattice. As a result, graphene growth on copper is self-limited, and formation of multilayer graphene is generally prohibited. Being able to control this process better, as well as the high quality produced, makes copper-based growth the dominating synthesis procedure in the graphene community. We designed a two-temperature zone system to spatially separate the catalytic decomposition step of carbon precursors and the surface graphitization step for breaking this self-limited growth feature, giving high-quality Bernal stacked bilayer graphene via van der Waals epitaxy. We performed the so-called wrinkle engineering by growing graphene on nanostructured copper foil together with a structure-preserved surface transfer. In such a way, we controlled the wrinkling or folding on graphene and further fabricated graphene nanoribbon arrays by self-masked plasma etching. Moreover, by designing a two-step patching growth process on copper, we succeeded in synthesizing the mosaic graphene, a patchwork of intrinsic and nitrogen-doped graphene connected by single crystalline graphene p−n junctions.

By following a general concept of process engineering, our work on the designed CVD growth of graphene and its 2D hybrids provides a unique insight of this research field. It enables the precise growth control of graphene together with the in-depth understanding of CVD growth process, which would further stimulate the pace of graphene applications.

Published on the Web 07/19/2013 www.pubs.acs.org/accounts
10.1021/ar400057n

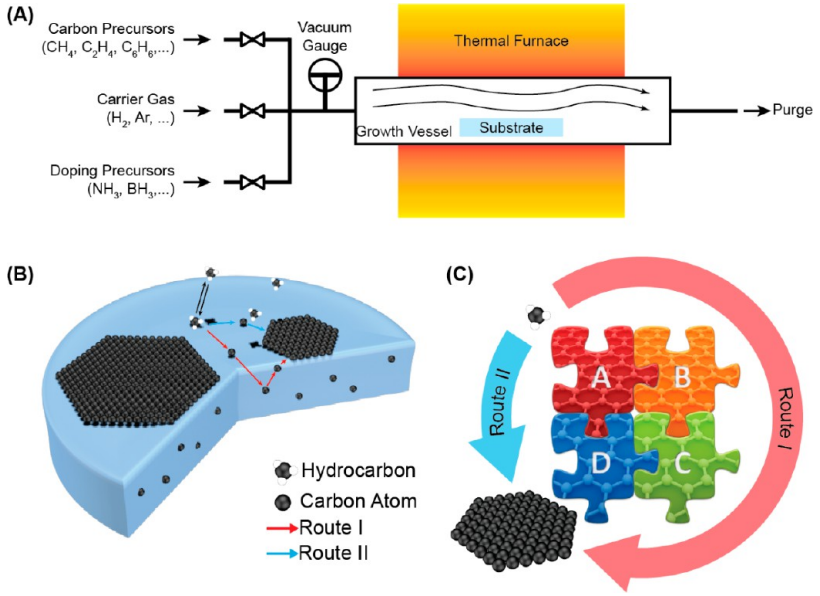

FIGURE 1. (A) Sketch drawing of a typical CVD system for designed growth of graphene. (B) Elementary steps involved in the CVD process. Red arrows represent the case for carbon-dissolvable substrate (route I), and the blue arrows demonstrate the case for carbon nondissolvable substrate (route II). (C) Schematic illustration for process engineering. Four elementary steps connected together for the synthesis of graphene. Two distinct routes coexist from hydrocarbon precursors to graphene.

1. Introduction

Graphene refers to a flat monolayer or a few layers of tightly packed carbon atoms arranged into two-dimensional (2D) honeycomb lattice.[1] Although it had been named and theoretically studied several decades ago,[2,3] graphene received little attention, until the detailed experimental studies conducted by Andrei Geim and his colleagues in 2004,[1] whose work triggered an explosion of interest in this star material. Since then, thousands of researchers were attracted by the fascinating properties of graphene, most of which arose from the unique linear dispersion relationship in the graphene band structure. Electrons in graphene behave as massless Dirac Fermions, which was confirmed by the experimental observation of half integer quantum Hall effects.[4,5] More importantly, room temperature carrier mobility in graphene was found to approach 200000 cm^2/V s, 2 orders of magnitude higher than silicon that currently dominates the semiconductor industry. The extraordinary performance in electronics is actually the strongest driving force for graphene research. On the other hand, the optical properties of graphene, as well as mechanical and thermal properties of graphene, are also outstanding.[6−9] The combination of all these excellent properties within the ultimate thickness makes graphene an excellent candidate material for not only future electronics[10] but also many other fields ranging from energy storage[11] to biotechnologies.[12]

However, the cost-effective production of graphene with high quality is crucial to its community. It was reported that in 2008, four years after its discovery, the price of a microsized piece of graphene even exceeded that of a 12 in. silicon wafer. The low yield of mechanical exfoliation from graphite would never meet the demand for large-scale production of graphene. As a result, alternative means for graphene synthesis with low cost and comparable quality is urgently required. Several different approaches were proposed, including graphitization of silicon carbide,[13] chemical reduction of graphite oxide,[14] liquid exfoliation of graphite,[15] and even organic synthesis,[16] etc. However, none of these methods was able to cover all critical issues for controllable synthesis, such as thickness, grain size, stacking order, defects, and doping. A breakthrough of graphene synthesis emerged after researchers revised early inspiring works in the late 1960s:[17,18] that high temperature treatment of certain metals in hydrocarbons could produce ultrathin graphitic films on the surface. By combining these old recipes with modern transfer printing technology,[19,20] chemical vapor deposition (CVD) of graphene was finally established.[21,22] After another four years of development, CVD is now able to synthesize graphene samples of acceptable quality.[23] Moreover, various kinds of transition metals, covering almost all the elements in VIIIB and IB groups, are capable for graphene growth.[24]

Despite all these prominent advances in CVD growth, in-depth understanding to this chemical process is actually lacking. The key factors governing a general CVD process include catalyst, precursor, flow rate, temperature, pressure, and time (Figure 1A). As a complex heterogeneous catalysis

system, the CVD process for graphene growth on metal can be simplified into four elementary steps: (A) adsorption and catalytic decomposition of precursor gas, (B) diffusion and dissolution of decomposed carbon species on the surface and into the bulk metal, (C) segregation of dissolved carbon atoms onto the metal surface, and finally (D) surface nucleation and growth of graphene (Figure 1B). As a matter of fact, for metals with poor affinity to carbon (e.g., Cu), another totally different route exists, in which dissolution and subsequent segregation of carbon atoms are prohibited.[25] In this case, the decomposition of hydrocarbon precursors was followed by direct formation of graphene, which is realized by diffusion of carbon atoms on the surface. The two routes are generally coexisting in all graphene CVD processes (Figure 1C), while their ratio strongly depends on the properties of metal substrate. Besides, among all the factors of the CVD system, metal substrate is the only one that is involved in all four elementary steps. It is, consequently, critical to initiate from designing the catalytic metal substrate in order to control the whole CVD process. Once the metal substrate is fixed, a designed enhancement or suppression of a specific elementary step would lead to graphene with a desired property, including thickness, grain size, bandgap, doping, and even hybridization with other 2D materials. According to this strategy, we were able to synthesize strict monolayer graphene,[26] few layer uniform graphene,[27−29] nitrogen-doped graphene,[30] bilayer Bernal graphene,[31] graphene nanoribbon arrays,[32] and mosaic graphene[33] with specific designed recipes. We would like to review these efforts in detail in this Account.

2. Process Engineering on Carbon Dissolvable Metals

Transition metals with incomplete d shells (e.g., Ni, Co, and Ru) usually exhibit a certain affinity to carbon, by either dissolving a considerable concentration of carbon or forming certain carbides. As a result, these metals provide a suitable platform to study these elementary steps, and more importantly, to improve the controllability of CVD growth. In this section, most of the design works were done with nickel, the earliest and most-studied carbon dissolvable substrate for graphene growth.

2.1. Segregation-Suppressed Monolayer Growth with Synergistic Bimetal Alloy. The major problem for graphene growth on nickel is the poor uniformity, since carbon dissolves into and precipitates out of a polycrystalline nickel substrate preferentially at defects and grain boundaries.[21] Plenty of work has been done in order to solve this problem, by either controlling the precursor flow or controlling the cooling rate.[34] These macroscopic solutions actually can hardly modify the microscopic processes during the growth. It is, consequently, nontrivial to solve this problem from a completely new point of view, by either restricting dissolution or segregation of carbon through process engineering. Since it is impossible to forbid carbon dissolution at high temperature, the segregation of carbon must be suppressed.

Carbide is an ideal solution for trapping dissolved carbon atoms. Although nickel carbide could easily decompose, compounds of carbon with IVB−VIB elements are considerably stable. Accordingly, a catalyst design based on a bimetal alloy was proposed. With this strategy, one component of the bimetal alloy serves for catalytic decomposition of the hydrocarbon precursor and surface graphitization, and the other component traps the dissolved carbon with stable carbides. As a result, the segregation step is fully forbidden, leading to strict monolayer graphene.

We chose molybdenum as a carbon trap, considering the easy accessibility and especially the high stability of its carbide (Figure 2A). Two-hundred nanometer nickel film was evaporated onto a 25 μm molybdenum foil as the substrate. The two components form a Ni−Mo alloy near the surface during the annealing process prior to graphene growth. Thereafter, the substrate undergoes a CVD growth procedure with exposure to methane at 1000 °C for 5 min. Revealed by transferring onto SiO_2/Si substrate, graphene film grown on the Ni−Mo alloy substrate exhibited extraordinary uniformity of the monolayer, without any trace of the few layers (Figure 2C). Raman spectroscopy of the sample exhibited no pronouncing D band (Figure 2E), and the carrier mobility could be as high as 973 cm^2/V s at room temperature (Figure 2F), both of which are indicative of high quality.

Different from the substrate with a single component, where the CVD growth depends on many experimental parameters (e.g., pressure, time, temperature, hydrocarbon feed and cooling rates), the designed procedure based on the bimetal alloy is extremely stable (Figure 2G), allowing massive production of uniform monolayer graphene. Moreover, the strategy can be extended to other bimetal alloys. We found that the carbon trapping metal (Mo) can be replaced with tungsten and vanadium, while the catalyst metal (Ni) can be chosen among cobalt and even iron. Every combination according to the strategy is confirmed to be capable for growth of strict monolayer graphene. Contemporaneous work also claimed efficient effects of the bimetal

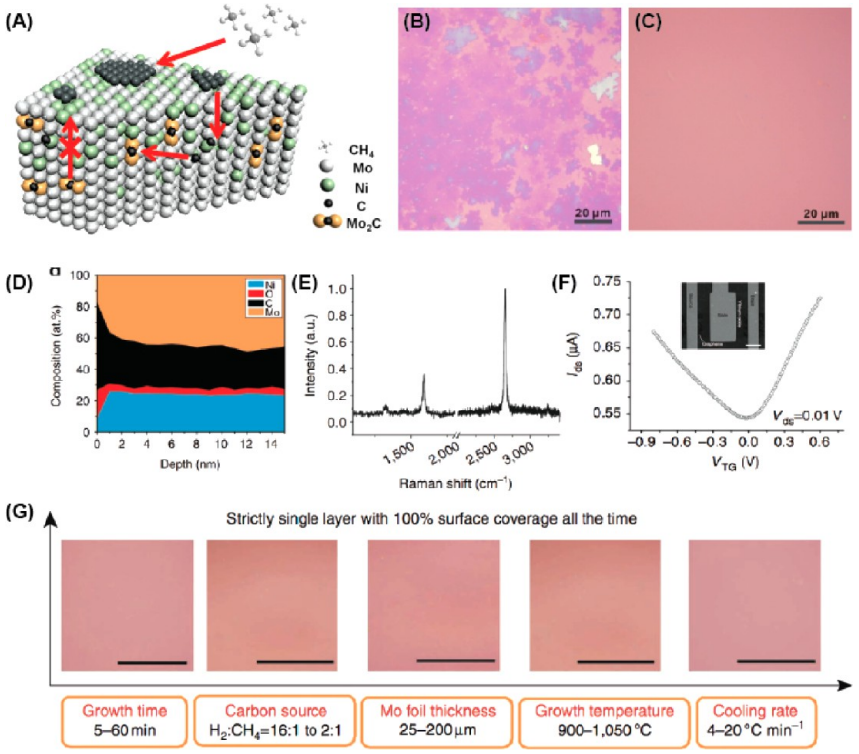

FIGURE 2. Strict monolayer graphene grown from synergistic bimetal alloy substrate. (A) Elementary steps involved in the process. (B and C) Optical microscope images of graphene grown on nickel and the Ni−Mo alloy, respectively. (D) XPS composition profiles of elements along the surface normal direction on the Ni−Mo substrate after graphene growth. (E) Raman spectrum of graphene grown on the Ni−Mo alloy. (F) Transfer characteristics of a top-gate graphene transistor. Inset: SEM image of the device. (G) Typical optical microscope images of graphene films grown on the Ni−Mo alloy with variations to growth parameters.

substrate on thickness control of graphene;[35] however, a distinct mechanism was involved. The introduction of the bimetal substrate provides a cost-effective route for controlled growth of graphene, as well as a new sight into the CVD process.

2.2. Segregation-Only Growth of Uniform Few Layer Graphene. Segregation refers to the enrichment of one constituent at a free surface or interface from the bulk phase. Segregation of carbon from the bulk metal not only is the last step in CVD growth but also is a ubiquitous phenomenon involved from steelmaking to catalyst deactivation. The basic idea of the segregation-only growth technique we developed is to squeeze these predissolved solid carbons out to construct graphene at the metal surface.[27,28] In comparison with the typical CVD process with four elementary steps, the segregation growth approach involves only two elementary steps, segregation and nucleation growth, which is closer to an equilibrium process.[18] It therefore gives a better controllability to the thickness and uniformity.

We chose nickel as a prototype substrate for segregation, considering the moderate carbon solubility.[27] Thin nickel film was evaporated onto the SiO_2/Si substrate with a commercial nickel target containing trace amounts of carbon. After a designed period of annealing in vacuum at 1000 °C, the sample was slowly cooled to room temperature (Figure 3A). In comparison with samples grown from the traditional CVD process, segregated graphene exhibited a much better uniformity (Figure 3B). This segregation approach is also more practical, since experimental parameters include only pressure and temperature. Hence, there is a big freedom for scaling up the segregation growth with excellent uniformity (Figure 3C). We further extended this approach to other carbon dissolving metals [e.g., cobalt and iron (Figure 3, panels D and E)], with minor modification to the growth parameters.

A synergistic bimetal alloy design is also proposed for the segregation-only growth,[28] by introduction of copper[22,25] to nickel film to form Ni−Cu alloy as the segregation substrate (Figure 4A). A 5.5 atom % ratio of nickel led to the coverage of monolayer graphene exceeding 95%. When the ratio was increased to 10.4%, coverage of bilayer graphene would be 89% (Figure 4B). A novel avenue for graphene thickness control is thus established.

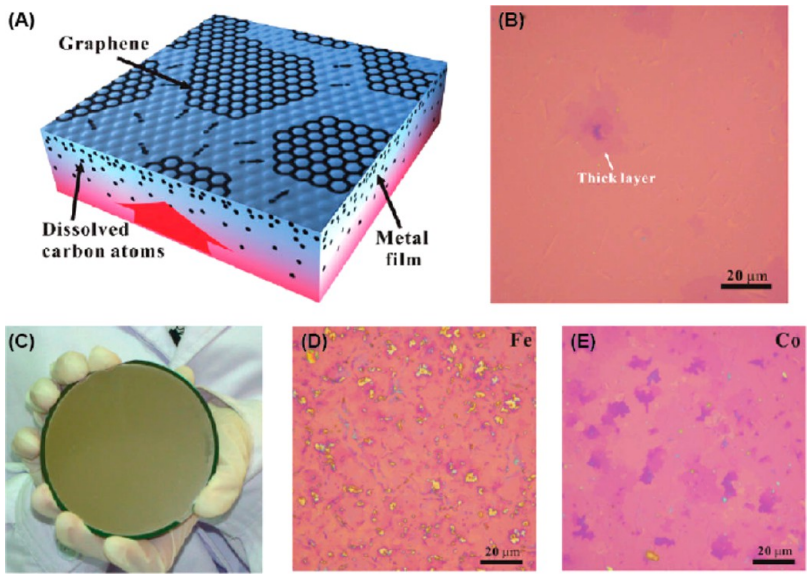

FIGURE 3. Segregation-only growth of graphene from nickel. (A) Schematic illustration of segregation technique, demonstrating the surface accumulation of buried carbon atoms in bulk metal and formation of graphene at high temperature. (B) Optical microscope image of segregated graphene transferred onto SiO_2/Si substrate. (C) Four inch graphene wafer segregated on polycrystalline Ni film. (D and E) Optical microscope images of graphene segregated from iron and cobalt, respectively.

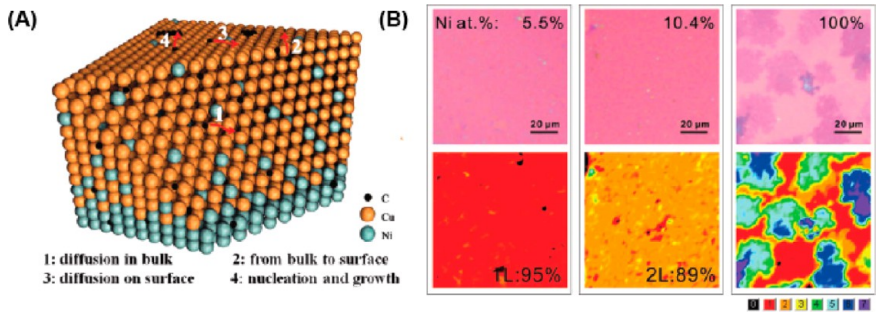

FIGURE 4. Layer-controlled segregation of graphene on synergistic Cu−Ni alloy substrate. (A) Schematic of the segregation process on the Cu−Ni alloy. (B) Optical microscope images of graphene segregated from Cu−Ni alloys with nickel atom concentration of 5.5%, 10.4%, and 100%, respectively. The bottom three panels indicated corresponding thickness analysis based on the optical contrast.

2.3. Cosegregation Growth of Doped Graphene. It is well-known in the semiconductor community that semiconductors need to be doped into n type or p type, in order to perform electronic functions. The situation is largely similar in graphene, which is aimed as a candidate for future electronics. However, doping of graphene is no longer facile, mainly because the traditional doping technique such as ion implantation fails to deal with the atomic thin film constructed by robust C−C bonds. Hence, it would be of great significance to develop a feasible manner for effective doping of graphene.[36,37] On the basis of the process engineering of graphene growth, we proposed a cosegregation route in which heteroatoms such as nitrogen and boron are introduced during the segregation.[30]

The substrate for cosegregation growth consists of three layers, as shown in Figure 5A. Similar to the previous case, nickel is responsible for the segregation of graphene.[27] Thanks to the feature of the segregation process, we are allowed to insert required dopants, such as nitrogen and boron within the substrate before they are squeezed out of the surface. Boron was embedded between nickel and the silicon wafer by evaporation, capturing a significant amount of nitrogen because of the high affinity of boron toward nitrogen.[38] During annealing, boron formed strong bonds with nickel,[39] while nitrogen would easily diffuse out of the surface, yielding nitrogen-doped graphene.

Cosegregated *n*-doped graphene was analyzed with various characterizations. There is a pronounced D-band corresponding to defects induced by doping in the Raman

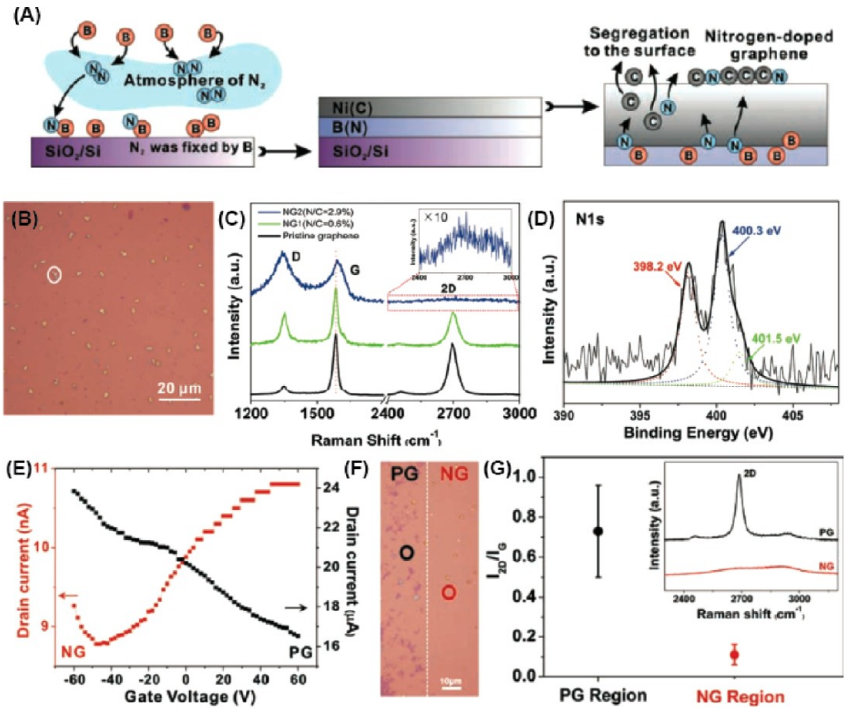

FIGURE 5. Cosegregation growth of N-doped graphene. (A) Experimental design of the cosegregation process. Nickel and boron served as a source of carbon and nitrogen, respectively. (B) Optical microscope image of cosegregated N-doped graphene. (C) Raman spectra of cosegregated N-doped graphene and traditional CVD graphene. (D) XPS N 1s spectrum of N-doped graphene. (E) Transfer characteristics of N-doped graphene, with comparison to that of pristine graphene with 0.5 V bias in vacuum. (F) Optical microscope image of graphene doped in the selected area (right). (G) Statistics on I_{2D}/I_G in the Raman spectra of n-doped and pristine graphene in the partially doped sample. 2D Bands collected in the circles in (E) are presented in the inset.

spectrum of N-doped graphene (Figure 5C). Importantly, X-ray photoelectron spectroscopy (XPS) reveals prominent concentration of nitrogen in graphitic, pyrrolic, and pyridinic forms, while boron is completely absent (Figure 5D). The N-doped graphene exhibited high uniformity, even comparable with that of intrinsic graphene (Figure 5B). Transport studies showed typical *n*-type behavior with the charge neutral point negatively shifted (Figure 5E). The resistance suffers from an exponential increase during temperature dropping, extracting a bandgap of 0.16 eV.

This doping approach allows for effective tuning of doping concentration, simply by adjusting the thickness of boron and nickel. We, accordingly, succeeded in controlling the concentration of nitrogen from 0.3 to 2.9 atom %. Besides, selected area doping is also applicable, as shown in Figure 5F. This cosegregation approach enables reliable large-area fabrication of doped graphene with a controlled doping concentration and region, both of which are crucial for potential graphene electronics.

2.4. Origin of Wrinkle Formation on CVD Graphene. CVD graphene usually exhibits corrugations or wrinkles of 2−15 nm, which is much larger than <1 nm of freestanding graphene.[40] The existence of these wrinkles actually limited the flatness of graphene, which further posed an obstacle for the process engineering of graphene growth. In order to address this problem, it is essential to understand the real origin of wrinkle formation. Our studies revealed that the morphology of the polycrystalline substrate plays a significant role in the formation of wrinkles.[29]

We employed nickel as the substrate for graphene growth, either by traditional CVD procedure or the segregation approach mentioned above. Synthesized graphene was transferred to SiO_2/Si by a transfer-printing technique.[19,20] During the transfer, surface morphology could also be preserved with high fidelity. As a result, direct morphological correlation between growth substrate and derived graphene can be performed (Figure 6, panels A and B). Extensive studies over the morphology indicate that two types of distinct wrinkles existed in transferred graphene. One type is the randomly distributed wrinkles with irregular shapes, attributable to the well-known thermal contraction. However, the other type of wrinkles also exists, shaped as closed circles with either a single edge or double edges, corresponding to isolated or neighbored grains of polycrystalline nickel

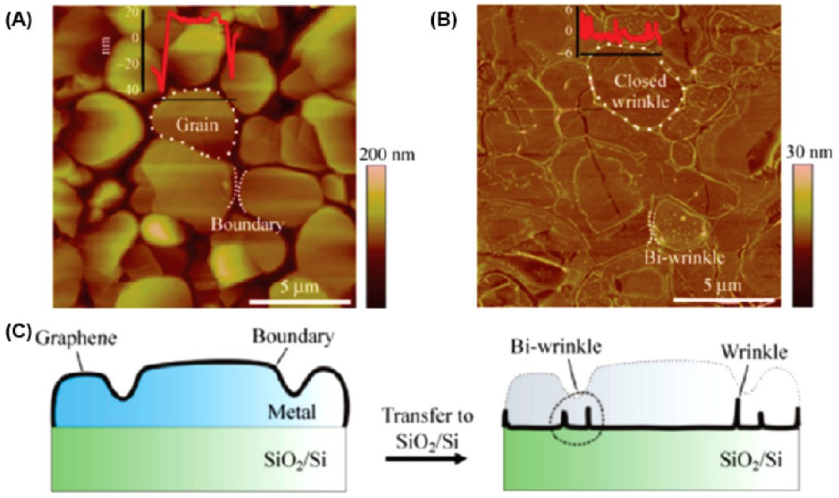

FIGURE 6. Wrinkle formation of graphene on nickel. (A) Atomic force microscope (AFM) image of polycrystalline nickel surface after graphene growth. (B) AFM image of graphene transferred onto SiO_2/Si substrate, where circled wrinkles can apparently be observed. (C) Schematic of wrinkle formation mechanism resulted from the polycrystalline nature of the growth substrate.

substrate. The shapes and the sizes of these circles are strongly correlated with the original growth substrate (Figure 6C). This result not only unveiled the origin of graphene wrinkles but also provided the potential of wrinkle engineering, which will be discussed later.

3. Process Engineering on Carbon Nondissolvable Metals

The behavior of metal substrate for graphene growth is mainly determined by its capability to dissolve carbon. Although most transition metals exhibit certain carbon solubility, elements with completely filled d shells (e.g., copper, silver and zinc, etc.) are definitely exceptions. The poor affinity of these elements to carbon makes the growth of graphene distinct from the case previously discussed, since carbon atoms could no longer diffuse into the bulk substrate. Graphene growth on copper was demonstrated as a successful example in this case, producing graphene with excellent uniformity of >95% monolayer.[22] From the aspect of process engineering, elementary steps of the growth for this situation are naturally simplified without dissolution and subsequent segregation. However, designed growth of graphene on carbon nondissolvable metals is still possible.

3.1. Bilayer Bernal Graphene via van der Waals Epitaxy. The major obstacle for graphene toward real application is the absence of an effective bandgap in its electronic structure. Several approaches were thus proposed and demonstrated in order to address this problem.[41−43] Among these approaches, it is facile to achieve a tunable bandgap by breaking the symmetry of Bernal-stacked bilayer graphene with a perpendicular electric field.[41,44] However, scalable synthesis of bilayer Bernal graphene is challenging. Few layer graphene grown on nickel usually lacks ordered stacking,[21,27] while copper suppresses formation of graphene other than the monolayer.[22] It is thus necessary to design a novel approach for the synthesis of bilayer graphene.[45]

Copper-based graphene growth could be viewed as two elementary steps, including adsorption and catalytic decomposition of hydrocarbon precursors, followed by graphene formation with diffusing carbon atoms. The forbidden growth of bilayer graphene arises from the fact that the first elementary step is disabled, once the copper surface is fully passivated by graphene. To break this behavior, we designed a two-zone CVD furnace for the purpose of spatially separating two elementary steps.[31] As illustrated in Figure 7A, a fresh copper foil was loaded to the upstream of the CVD tube for decomposing the hydrocarbons into fragments. Therefore, despite the passivated substrate downstream, the fresh copper foil could continue to provide decomposed carbon fragments to the existing monolayer graphene, where van der Waals epitaxy occurs to form bilayer graphene with ordered stacking.

After optimization to the growth parameters, the bilayer coverage of the synthesized graphene could reach 67% (Figure 7C). The sample was further characterized by Raman spectroscopy and electron diffraction, both of which revealed clear evidence for Bernal stacking. Moreover,

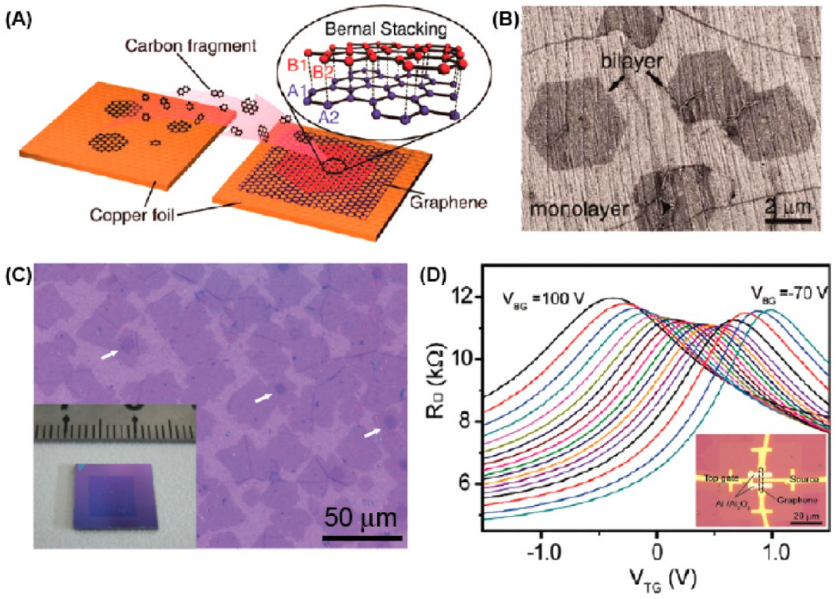

FIGURE 7. Formation of bilayer Bernal graphene on copper. (A) Schematic of the experimental setup and the growth mechanism. (B) SEM image of hexagonal bilayer graphene grains with identical orientation after epitaxial growth. (C) Optical microscope image of synthesized bilayer graphene with bilayer coverage over 67%. Inset: large area bilayer graphene after transfer. (D) Transfer characteristics of bilayer graphene device at various back gate voltages. The image of the device is shown in the inset.

synthesized bilayer graphene was embedded into dual-gated graphene transistors. In addition to the high mobility of 350−550 cm^2/V s, the device also exhibited a tunable on−off ratio that is controlled by the applied electric field (Figure 7D). These results indicate high quality and reliability of the designed approach for growth of bilayer Bernal graphene.

3.2. Wrinkle Engineering for Fabricating Graphene Nanoribbon Arrays. The quantum confinement effect can be utilized as an alternative way to achieve a bandgap in graphene. When graphene is narrowed into ribbons of <10 nm, a width-dependent bandgap would emerge, as first predicted by theoretical studies[46] and confirmed by experimental works.[42,43] However, there are still great technical challenges, mainly due to the difficulties in nanofabrication on the large scale. We proposed a fresh solution based on the concept of wrinkle engineering.[32] While the scalability is guaranteed by the essence of CVD, the wrinkled graphene can directly be converted to graphene nanoribbon arrays via self-masked plasma etching.

As previously discussed, graphene film grow continuously on a copper surface. Thus, the structural corrugations of the copper surface are cloned to graphene. Our work indicated that these structural features could mostly be preserved after transferred to a flat substrate via a careful transfer-printing operation.[32] As a result, the wrinkle structure on the monolayer graphene can be designed simply by nanostructuring the growth substrate, namely wrinkle engineering. As a matter of fact, there are plenty of parallel steps with typical heights of 20−30 nm formed on copper after the growth of graphene, arising from the sublimation and crystallization of copper,[47] as well as rolling lines in copper foil. These steps can be accordingly transformed into arrays of parallel graphene wrinkles as narrow as 10 nm, with three folds of graphene layers (Figure 8A). We further treated these wrinkle arrays with gentle plasma etching, during which monolayer graphene between wrinkles and the top layer graphene of wrinkles are eliminated, leaving well-aligned graphene nanoribbon arrays (Figure 8, panels B−D).

The as-prepared graphene nanoribbons exhibited an on−off ratio over 30 at room temperature, corresponding to an energy gap of ~100 meV (Figure 8F). More importantly, it is feasible to tune the density of graphene nanoribbons. As a demonstration, we successfully synthesized graphene nanoribbon arrays with various densities. Obviously, our wrinkle engineering-based approach provides a scalable and controllable manner for batch fabrication of highly aligned graphene nanoribbon arrays, which may open up a new pathway for graphene electronics.

3.3. Mosaic Graphene and Modulation-Doped Growth. The graphene p−n junction is attracting wide attention, arising from its promising performance in photoelectric conversion[48,49] and electron optics.[50] However, traditional

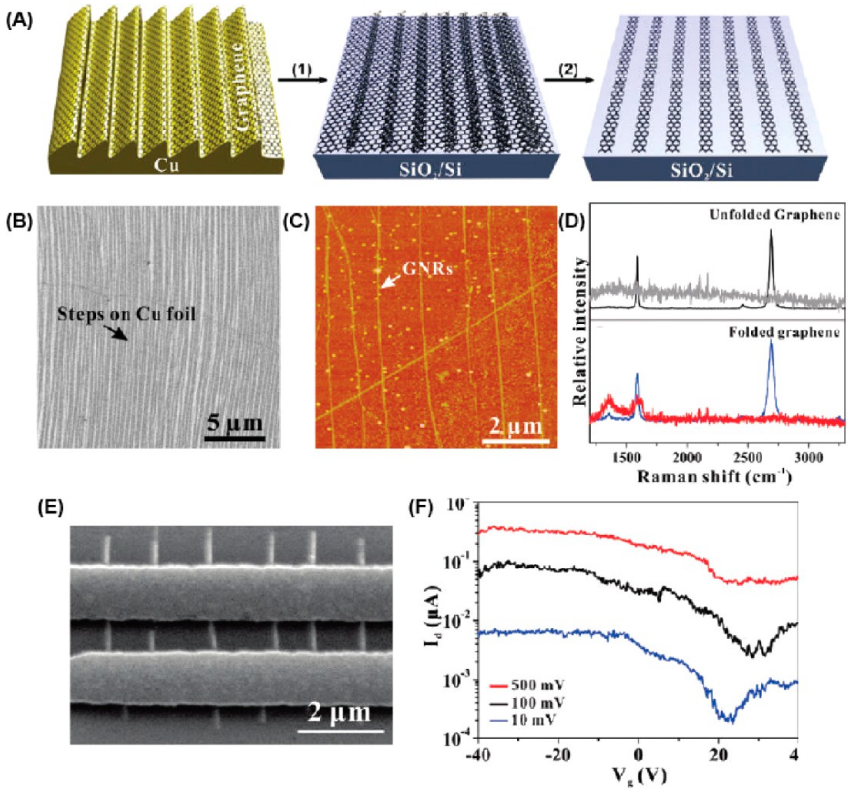

FIGURE 8. Large-scale graphene nanoribbon arrays based on wrinkle engineering growth. (A) Schematic of the processes for fabrication of graphene nanoribbon arrays. (B) SEM image of copper surface after graphene growth, indicating massive parallel steps. (C) AFM image of as-fabricated graphene nanoribbons. (D) Raman spectra of unfolded (up) and folded (down) graphene, before and after plasma etching, respectively. (E) SEM image of a back-gated transistor with a graphene nanoribbon array. (F) Transfer characteristics of graphene nanoribbon array device at various biases.

means for fabrication of graphene p–n junctions is either complicated[49] or unstable,[51] while no solution is yet scalable. Considering that the final elementary step in CVD growth of graphene on copper is restricted by self-limiting effect, we proposed a novel lateral modulation-doped procedure for the growth of mosaic graphene, an in-plane hybrid structure of intrinsic and doped graphene (Figure 9A), which are connected by single crystalline p–n junctions within the atomic thickness.[33]

The modulation-doped CVD growth was initiated with substrate annealing and nucleation of intrinsic grains, similar to the normal procedure on copper. However, the growth was halted before the coalescence of discrete grains. The gaps between these grains were delicately controlled according to the nucleation density. Instead of methane, acetonitrile vapor was later introduced as the single precursor for nitrogen-doped graphene. During this step, active edges of intrinsic graphene grains served as nucleation sites for nitrogen-doped graphene, resulting in single-crystalline graphene p–n junctions. This strategy was further proven to be applicable for multicycle modulation, as well as scaling up (Figure 9, panels B and C).

The as-grown graphene film is rather uniform in thickness, as indicated by the optical microscope and AFM. However, the distinct feature of intrinsic and nitrogen-doped portions could easily be revealed by the scanning electron microscope (Figure 9D) and Raman mapping (Figure 9E). Extensive electron diffraction studies confirmed the single-crystalline nature of graphene p–n junctions. Because of the improved growth procedure, both of the two portions exhibited outstanding mobility, which could reach 2500 cm^2/V s and 5000 cm^2/V s for the nitrogen-doped and intrinsic portion, respectively (Figure 9F). Most importantly, carrier-dependent photocurrent dominated by the photothermoelectric (PTE) effect[48,49] was observed at the graphene p–n junction (Figure 9G). This progress enabled large-scale integration of graphene-based electronic and photoelectronic circuits.

4. Summary and Outlooks

The explosive development of CVD growth of graphene calls for an in-depth understanding of its elementary steps, which are essential for both fundamental research and practical applications. In this Account, our recent progress

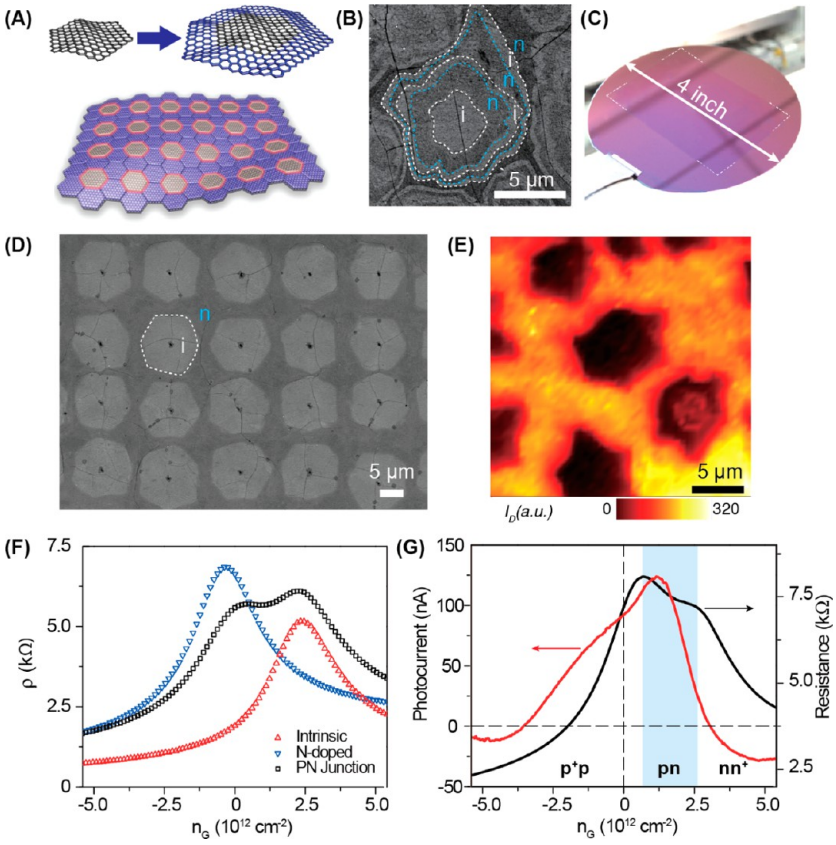

FIGURE 9. Modulation-doped growth of mosaic graphene. (A) Schematic drawing of modulation-doped growth and mosaic graphene. (B) SEM image of synthesized graphene with three modulation cycles. (C) Large area mosaic graphene transferred onto a 4 in. silicon wafer. (D) SEM image of periodic mosaic graphene. (E) D band mapping of Raman spectroscopy over a certain area of mosaic graphene. (F) Transport properties of mosaic graphene, including intrinsic and nitrogen-doped portions, as well as the p−n junction. (G) Transfer characteristic (black) and photoelectric property (red) of the p−n junction in mosaic graphene.

toward designed CVD growth of graphene with the guidance of process engineering is reviewed in detail. A typical CVD process could be divided into four individual elementary steps. We succeeded in designing these elementary steps for enhanced controllability of the whole growth process with typical cases involving both carbon dissolvable and nondissolvable substrates.

Although CVD growth is almost the most successful route for large area synthesis of graphene, potential challenges still exist. The next critical step of graphene growth relies on more precise control of its elementary steps. For instance, ideal graphene materials should exhibit as large area single crystals. Despite a few recent progresses addressing this problem,[52] underlying mechanism of graphene nucleation is still to be unveiled. This requires deeper comprehension to the elementary steps, especially the segregation process that directly determines density of graphene grains. Furthermore, it would be of great attraction if direct growth on the insulating substrate could be enabled. Implementation of information gained based on process engineering to insulating materials such as glass and ceramics may be a potential route for this target.

The work was supported by the Natural Science Foundation of China (Grants 51290272, 51121091, 51072004) and the Ministry of Science and Technology of China (Grants 2013CB932603, 2012CB933404, 2011CB933003).

BIOGRAPHICAL INFORMATION

Dr. Kai Yan received both his B.S. in physics in 2007 and his Ph.D. in physical chemistry in 2012 from Peking University, working on designed CVD growth of graphene as well as electronic device applications based on CVD graphene. Presently, he is a postdoctoral scholar at Stanford University.

Dr. Lei Fu received his B.S. degree in chemistry from Wuhan University in 2001. He obtained his Ph.D. degree from the Institute of Chemistry, Chinese Academy of Sciences, in 2006. After obtaining his Ph.D., he worked as a Director's Postdoctoral Fellow at the Los Alamos National Laboratory, Los Alamos, NM (2006−2007). Thereafter, he became an associate professor of Peking University. In 2012, he joined Wuhan University as a full professor.

His research interests cover two-dimensional materials and flexible devices.

Dr. Hailin Peng received his B.S. in chemistry from Jilin University in 2000 and a Ph.D. in physical chemistry from Peking University in 2005. After his postdoctoral studies at Stanford University during 2005−2009, he became an associate professor of Peking University in 2009. Currently, his research interest is focused on controlled growth, chemical modifications, heterostructures, and optoelectronic devices of 2D materials.

Dr. Zhongfan Liu received his Ph.D. from the University of Tokyo in 1990. After a postdoctoral fellowship at the Institute for Molecular Science, Japan, he became an associate professor (1993), full professor (1993), and Cheung Kong Chair professor (1999) of Peking University. He was elected as a member of the Chinese Academy of Sciences in 2011. He is now the Director of the Institute of Physical Chemistry, Center for Nanoscale Science and Technology, and Center for Nanochemistry of Peking University. His research interest is focused on low-dimensional carbon materials and novel 2D atomic crystals targeting nanoelectronic and energy conversion devices together with the exploration of fundamental phenomena in nanoscale systems.

FOOTNOTES

The authors declare no competing financial interest.

REFERENCES

1 Novoselov, K. S.; Geim, A. K.; Morozov, S. V.; Jiang, D.; Zhang, Y.; Dubonos, S. V.; Grigorieva, I. V.; Firsov, A. A. Electric field effect in atomically thin carbon films. *Science* **2004**, *306*, 666–669.

2 Boehm, H. P.; Clauss, A.; Fischer, G. O.; Hofmann, U. Das Adsorptionsverhalten sehr dünner Kohlenstoff-Folien. *Zeitschrift für Anorganische und Allgemeine Chemie* **1962**, *316*, 119–127.

3 Wallace, P. R. The band theory of graphite. *Phys. Rev.* **1947**, *71*, 622–634.

4 Novoselov, K. S.; Geim, A. K.; Morozov, S. V.; Jiang, D.; Katsnelson, M. I.; Grigorieva, I. V.; Dubonos, S. V.; Firsov, A. A. Two-dimensional gas of massless Dirac fermions in graphene. *Nature* **2005**, *438*, 197–200.

5 Zhang, Y.; Tan, Y.-W.; Stormer, H. L.; Kim, P. Experimental observation of the quantum Hall effect and Berry's phase in graphene. *Nature* **2005**, *438*, 201–204.

6 Nair, R. R.; Blake, P.; Grigorenko, A. N.; Novoselov, K. S.; Booth, T. J.; Stauber, T.; Peres, N. M. R.; Geim, A. K. Fine structure constant defines visual transparency of graphene. *Science* **2008**, *320*, 1308–1308.

7 Balandin, A. A.; Ghosh, S.; Bao, W.; Calizo, I.; Teweldebrhan, D.; Miao, F.; Lau, C. N. Superior thermal conductivity of single-layer graphene. *Nano Lett.* **2008**, *8*, 902–907.

8 Lee, C.; Wei, X.; Kysar, J. W.; Hone, J. Measurement of the elastic properties and intrinsic strength of monolayer graphene. *Science* **2008**, *321*, 385–388.

9 Ghosh, S.; Bao, W.; Nika, D. L.; Subrina, S.; Pokatilov, E. P.; Lau, C. N.; Balandin, A. A. Dimensional crossover of thermal transport in few-layer graphene. *Nat. Mater.* **2010**, *9*, 555–558.

10 Schwierz, F. Graphene transistors. *Nature Nanotechnol.* **2010**, *5*, 487–496.

11 Zhu, Y.; Murali, S.; Stoller, M. D.; Ganesh, K. J.; Cai, W.; Ferreira, P. J.; Pirkle, A.; Wallace, R. M.; Cychosz, K. A.; Thommes, M.; Su, D.; Stach, E. A.; Ruoff, R. S. Carbon-based supercapacitors produced by activation of graphene. *Science* **2011**, *332*, 1537–1541.

12 Garaj, S.; Hubbard, W.; Reina, A.; Kong, J.; Branton, D.; Golovchenko, J. A. Graphene as a subnanometre trans-electrode membrane. *Nature* **2010**, *467*, 190–193.

13 Berger, C.; Song, Z.; Li, T.; Li, X.; Ogbazghi, A. Y.; Feng, R.; Dai, Z.; Marchenkov, A. N.; Conrad, E. H.; First, P. N.; de Heer, W. A.; Nanoelectronics, G.-b.; Heer, W. A. D. Ultrathin epitaxial graphite: 2D Electron gas properties and a route toward graphene-based nanoelectronics. *J. Phys. Chem. B* **2004**, *108*, 19912–19916.

14 Stankovich, S.; Dikin, D. A.; Dommett, G. H. B.; Kohlhaas, K. M.; Zimney, E. J.; Stach, E. A.; Piner, R. D.; Nguyen, S. T.; Ruoff, R. S. Graphene-based composite materials. *Nature* **2006**, *442*, 282–286.

15 Li, D.; Muller, M. B.; Gilje, S.; Kaner, R. B.; Wallace, G. G. Processable aqueous dispersions of graphene nanosheets. *Nature Nanotechnol.* **2008**, *3*, 101–105.

16 Yang, X.; Dou, X.; Rouhanipour, A.; Zhi, L.; Räder, H. J.; Müllen, K. Two-dimensional graphene nanoribbons. *J. Am. Chem. Soc.* **2008**, *130*, 4216–4217.

17 Robertson, S. D. Graphite formation from low temperature pyrolysis of methane over some transition metal surfaces. *Nature* **1969**, *221*, 1044–1046.

18 Shelton, J. C.; Patil, H. R.; Blakely, J. M. Equilibrium segregation of carbon to a nickel (111) surface: A surface phase transition. *Surf. Sci.* **1974**, *43*, 493–520.

19 Jiao, L.; Fan, B.; Xian, X.; Wu, Z.; Zhang, J.; Liu, Z. Creation of nanostructures with poly(methyl methacrylate)-mediated nanotransfer printing. *J. Am. Chem. Soc.* **2008**, *130*, 12612–12613.

20 Reina, A.; Son, H.; Jiao, L.; Fan, B.; Dresselhaus, M. S.; Liu, Z.; Kong, J. Transferring and identification of single- and few-layer graphene on arbitrary substrates. *J. Phys. Chem. C* **2008**, *112*, 17741–17744.

21 Reina, A.; Jia, X.; Ho, J.; Nezich, D.; Son, H.; Bulovic, V.; Dresselhaus, M. S.; Kong, J. Large area, few-layer graphene films on arbitrary substrates by chemical vapor deposition. *Nano Lett.* **2009**, *9*, 30–35.

22 Li, X.; Cai, W.; An, J.; Kim, S.; Nah, J.; Yang, D.; Piner, R.; Velamakanni, A.; Jung, I.; Tutuc, E.; Banerjee, S. K.; Colombo, L.; Ruoff, R. S. Large-area synthesis of high-quality and uniform graphene films on copper foils. *Science* **2009**, *324*, 1312–1314.

23 Li, X.; Magnuson, C. W.; Venugopal, A.; An, J.; Suk, J. W.; Han, B.; Borysiak, M.; Cai, W.; Velamakanni, A.; Zhu, Y.; Fu, L.; Vogel, E. M.; Voelkl, E.; Colombo, L.; Ruoff, R. S. Graphene films with large domain size by a two-step chemical vapor deposition process. *Nano Lett.* **2010**, *10*, 4328–4334.

24 Bartelt, N. C.; McCarty, K. F. Graphene growth on metal surfaces. *MRS Bull.* **2012**, *37*, 1158–1165.

25 Li, X.; Cai, W.; Colombo, L.; Ruoff, R. S. Evolution of graphene growth on Ni and Cu by carbon isotope labeling. *Nano Lett.* **2009**, *9*, 4268–4272.

26 Dai, B.; Fu, L.; Zou, Z.; Wang, M.; Xu, H.; Wang, S.; Liu, Z. Rational design of a binary metal alloy for chemical vapour deposition growth of uniform single-layer graphene. *Nat. Commun.* **2011**, *2*, 522.

27 Liu, N.; Fu, L.; Dai, B.; Yan, K.; Liu, X.; Zhao, R.; Zhang, Y.; Liu, Z. Universal segregation growth approach to wafer-size graphene from non-noble metals. *Nano Lett.* **2011**, *11*, 297–303.

28 Liu, X.; Fu, L.; Liu, N.; Gao, T.; Zhang, Y.; Liao, L.; Liu, Z. Segregation Growth of Graphene on Cu−Ni Alloy for Precise Layer Control. *J. Phys. Chem. C* **2011**, *115*, 11976–11982.

29 Liu, N.; Pan, Z.; Fu, L.; Zhang, C.; Dai, B.; Liu, Z. The origin of wrinkles on transferred graphene. *Nano Res.* **2011**, *4*, 996–1004.

30 Zhang, C.; Fu, L.; Liu, N.; Liu, M.; Wang, Y.; Liu, Z. Synthesis of nitrogen-doped graphene using embedded carbon and nitrogen sources. *Adv. Mater.* **2011**, *23*, 1020–1024.

31 Yan, K.; Peng, H.; Zhou, Y.; Li, H.; Liu, Z. Formation of bilayer bernal graphene: Layer-by-layer epitaxy via chemical vapor deposition. *Nano Lett.* **2011**, *11*, 1106–1110.

32 Pan, Z.; Liu, N.; Fu, L.; Liu, Z. Wrinkle engineering: A new approach to massive graphene nanoribbon arrays. *J. Am. Chem. Soc.* **2011**, *133*, 17578–17581.

33 Yan, K.; Wu, D.; Peng, H.; Jin, L.; Fu, Q.; Bao, X.; Liu, Z. Modulation-doped growth of mosaic graphene with single-crystalline p-n junctions for efficient photocurrent generation. *Nat. Commun.* **2012**, *3*, 1280.

34 Reina, A.; Thiele, S.; Jia, X.; Bhaviripudi, S.; Dresselhaus, M.; Schaefer, J.; Kong, J. Growth of large-area single- and Bi-layer graphene by controlled carbon precipitation on polycrystalline Ni surfaces. *Nano Res.* **2009**, *2*, 509–516.

35 Park, J.-U.; Nam, S.; Lee, M.-S.; Lieber, C. M. Synthesis of monolithic graphene−graphite integrated electronics. *Nat. Mater.* **2012**, *11*, 120–125.

36 Wang, X.; Li, X.; Zhang, L.; Yoon, Y.; Weber, P. K.; Wang, H.; Guo, J.; Dai, H. N-Doping of graphene through electrothermal reactions with ammonia. *Science* **2009**, *324*, 768–771.

37 Wei, D.; Liu, Y.; Wang, Y.; Zhang, H.; Huang, L.; Yu, G. Synthesis of N-doped graphene by chemical vapor deposition and its electrical properties. *Nano Lett.* **2009**, *9*, 1752–1758.

38 Konno, H.; Nakahashi, T.; Inagaki, M.; Sogabe, T. Nitrogen incorporation into boron-doped graphite and formation of B−N bonding. *Carbon* **1999**, *37*, 471–475.

39 Xu, J.; Saeys, M. Improving the coking resistance of Ni-based catalysts by promotion with subsurface boron. *J. Catal.* **2006**, *242*, 217–226.

40 Meyer, J. C.; Geim, A. K.; Katsnelson, M. I.; Novoselov, K. S.; Booth, T. J.; Roth, S. The structure of suspended graphene sheets. *Nature* **2007**, *446*, 60–63.

41 Ohta, T.; Bostwick, A.; Seyller, T.; Horn, K.; Rotenberg, E. Controlling the electronic structure of bilayer graphene. *Science* **2006**, *313*, 951–954.

42 Han, M. Y.; Ozyilmaz, B.; Zhang, Y.; Kim, P. Energy band-gap engineering of graphene nanoribbons. *Phys. Rev. Lett.* **2007**, *98*, 206805–206809.

43 Li, X.; Wang, X.; Zhang, L.; Lee, S.; Dai, H. Chemically derived, ultrasmooth graphene nanoribbon semiconductors. *Science* **2008**, *319*, 1229–1232.

44 Castro, E. V.; Novoselov, K. S.; Morozov, S. V.; Peres, N. M. R.; dos Santos, J. M. B. L.; Nilsson, J.; Guinea, F.; Geim, A. K.; Neto, A. H. C. Biased bilayer graphene: Semiconductor with a gap tunable by the electric field effect. *Phys. Rev. Lett.* **2007**, *99*, 216802–216806.

45 Liu, L.; Zhou, H.; Cheng, R.; Yu, W. J.; Liu, Y.; Chen, Y.; Shaw, J.; Zhong, X.; Huang, Y.; Duan, X. High-yield chemical vapor deposition growth of high-quality large-area AB-stacked bilayer graphene. *ACS Nano* **2012**, *6*, 8241–8249.

46 Son, Y.-W.; Cohen, M. L.; Louie, S. G. Energy gaps in graphene nanoribbons. *Phys. Rev. Lett.* **2006**, *97*, 216803–216807.

47 Wofford, J. M.; Nie, S.; McCarty, K. F.; Bartelt, N. C.; Dubon, O. D. Graphene islands on Cu foils: The interplay between shape, orientation, and defects. *Nano Lett.* **2010**, *10*, 4890–4896.

48 Song, J. C. W.; Rudner, M. S.; Marcus, C. M.; Levitov, L. S. Hot Carrier Transport and Photocurrent Response in Graphene. *Nano Lett.* **2011**, *11*, 4688–4692.

49 Gabor, N. M.; Song, J. C. W.; Ma, Q.; Nair, N. L.; Taychatanapat, T.; Watanabe, K.; Taniguchi, T.; Levitov, L. S.; Jarillo-Herrero, P. Hot carrier—assisted intrinsic photoresponse in graphene. *Science* **2011**, *334*, 648–652.

50 Cheianov, V. V.; Fal'ko, V.; Altshuler, B. L. The focusing of electron flow and a veselago lens in graphene p-n junctions. *Science* **2007**, *315*, 1252–1255.

51 Lohmann, T.; von Klitzing, K.; Smet, J. H. Four-terminal magneto-transport in graphene p-n junctions created by spatially selective doping. *Nano Lett.* **2009**, *9*, 1973–1979.

52 Yan, Z.; Lin, J.; Peng, Z.; Sun, Z.; Zhu, Y.; Li, L.; Xiang, C.; Samuel, E. L.; Kittrell, C.; Tour, J. M. Toward the synthesis of wafer-scale single-crystal graphene on copper foils. *Acs Nano* **2012**, *6*, 9110–9117.